Understanding Correlation of Peculiar Velocity Vectors in the Cosmicflows-3 Database

by

Kristian D. Barajas

Submitted in Partial Fulfillment of the
Requirements for the Degree

Bachelor of Arts

Supervised by
Dr. Rick Watkins

Department of Physics

Willamette University, College of Liberal Arts
Salem, Oregon

2018

Presentations and publications

Senior Seminar Fall 2016 Presentations

Acknowledgments

Thanks to everyone!

Abstract

My abstract goes here.

Table of Contents

List of Tables

List of Figures

1   Introduction

In localized regions of space, smaller scale influences such as gravitational attraction dominate pulling matter towards regions of higher density. A simple example of this would be a galaxy being pulled towards a larger, more massive galaxy. While this behavior is most certainly still present at scales much larger than individual galaxies, the "motion" that dominates in this realm is due cosmological expansion which is often referred to more simply as the "stretching" of space between objects. While the driving factor for this large scale motion is still in principle due to gravity, what we see is that objects in space are being stretched away from each other often faster than they are moving toward regions of higher density. However, the motion towards regions of higher density at large scales can be seen as deviations from an idealized isotropic model of cosmological expansion. These aberrations in the model that indicate large scale flows in contrast to the linear growth of the universe can tell us more about the origin of the universe from the Big Bang and what the behavior of the universe may look like in the future. In this thesis we concern ourselves with the influence of the deviations from the model of cosmological expansion and propose a method to adequately model the large scale motions of the universe.

2 Background

In this section I will provide the precursory background knowledge on how spectroscopic and photometric measurements of galaxies, Cepheid variable stars, and supernovae type Ia lead to an idealized cosmological model. Subsequently, I will show how deviations from the model can be used to draw understanding of large scale motion in the universe.

2.0.1 Measuring Redshift through Spectroscopy

Each atom has a unique spectrum of emission and absorption lines from which astronomers may draw useful information from spectroscopic measurements, such as the composition and velocity of an astronomical object. This is accomplished by comparing the position of the spectral lines of a specified element observed in a given object against those measured in Earth's rest frame. Any measured increase in wavelength against the reference spectrum appears as a *redshift* towards longer, "redder" wavelengths, while a measured decrease appears as a *blueshift* towards shorter, "bluer" wavelengths (see Fig. 2.1) [Spe]. A classic example of this phenomenon is known as the Doppler effect, where a stationary observer experiences a change in pitch when an ambulence (the source of sound waves) approaches producing the effect of a higher frequency and shorter wavelength and then recedes with the converse effect, representing a blueshift and redshift respectively. To a first approximation, we can use the Doppler effect to express observed shifts in spectral lines as follows:

$$z \equiv \frac{\lambda_o}{\lambda_{\text{rest}}} - 1 = \frac{\Delta\lambda}{\lambda_{\text{rest}}} \tag{2.1}$$

where z is the redshift[1], λ_o is the spectral line as observed from the astronomical object, λ_{rest} is the spectral line as measured in Earth's rest frame, and $\Delta\lambda$ is the shift between λ_o and λ_{rest} [Hog99; Moo12].

---

[1]It should be noted that based on our definition a negative redshift is equivalent to an observed blueshift.
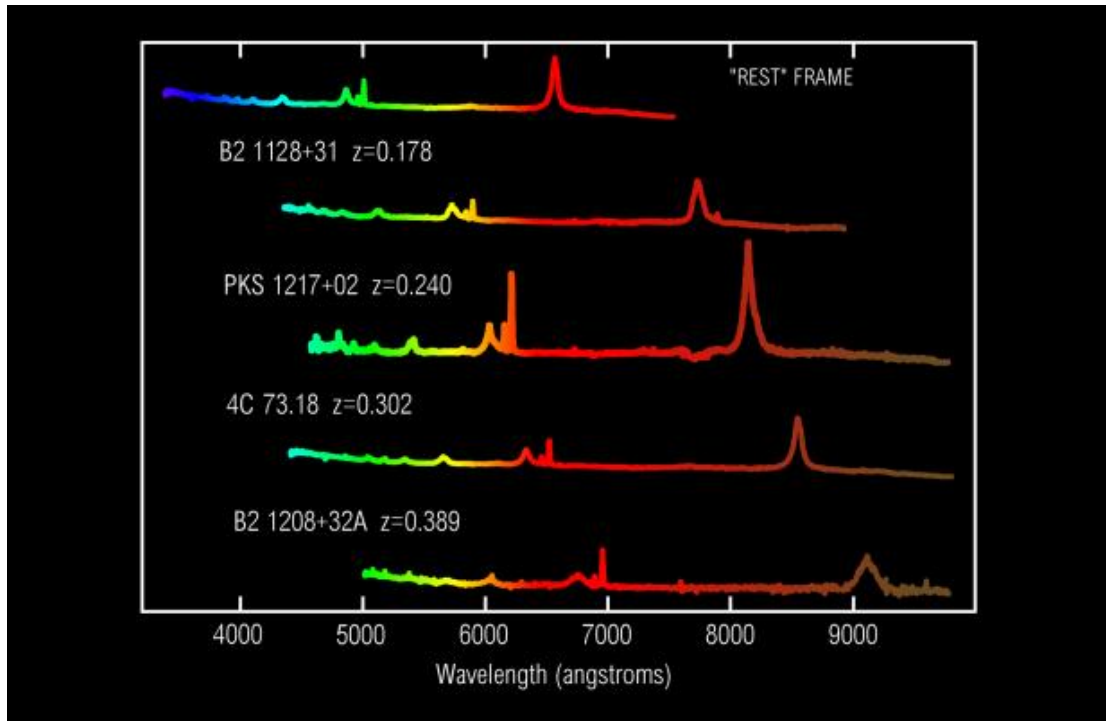
Figure 2.1: Hydrogen Spectra of Quasi-Stellar Objects (QSO) Exhibiting Redshift [Spe]. The first spectrum is an example of a QSO in a theoretical "rest frame" with no motion with respect to Earth. The subsequent spectra are of four different QSOs in order of increasing redshift away from Earth. While the hydrogen lines shift to longer, "redder" wavelengths, the spacing in the spectral lines remains the same between spectra.

2.0.2   Measuring Distance through Luminosity

NEEDS OVERVIEW OF THE STANDARD CANDLE METHOD OF DISTANCE MEASUREMENT

The most precise method of measuring distance to a galaxy is by measuring the luminosity of Type Ia supernovae [BT92; GP95]. However, supernova Type Ia are quite rare as they are only known to occur around once every one hundred years in a galaxy. The reason that Type Ia supernovae are often sought after and used as standard candles of distance is due to the fact that they only occur when a white dwarf star explodes from accruing mass until it has reached its maximum size of 1.44 solar masses, known as the Chandrasekhar limit. After this point, the star will suddenly explode in a highly predictable manner as a Type Ia supernova [Car01; KGC+05; NRT+16]. Because we know that all white dwarfs must overcome a critical mass in order for a supernova to occur, models have been used to accurately predict the behavior of the explosion based on the principle that nearly all Type Ia

supernova begin roughly at the same mass, size, and composition [GP95]. Using photometry we can measure the apparent magnitude or the brightness as seen on Earth over time, otherwise known as the light curve, of a Type Ia supernova. From the models we can usually accurately predict the luminosity or absolute magnitude of a Type Ia supernova, which is a standard measurement of the brightness of an object as seen from 10 parsecs away [RSC+07]. Given these measurements we can calculate the luminosity distance D_L of a Type Ia supernova from the distance modulus equation:

$$m = M + 5\log[D_L] + K + 25 \tag{2.2}$$

where m is the apparent magnitude, M is the absolute magnitude, and K is a correction term due to redshifting [Car01; NRT+16].

2.0.3 Hubble's Law and Hubble constant

We can then relate the redshift to the velocity of the object receding away from us through the relativistic Doppler effect as follows:

$$z = \sqrt{\frac{1 + v/c}{1 - v/c}} - 1 \tag{2.3}$$

where v is the line-of-sight radial velocity of the object and c is the speed of light [Hog99; Kir04; Moo12]. And, in the limiting case where the radial velocity is much less than the speed of light, the equation reduces to

$$z \approx \frac{v}{c} \tag{2.4}$$

which is the relationship used to relate the redshift in the spectral lines to the radial velocity of a galaxy [Hog99; Moo12].

Given measurements of the redshift and distances from Type Ia supernova surveys, astronomers can plot the radial velocity as a function of distance as seen in Fig. 2.2 [Kir04]. Again, using the limiting case where the radial velocity v is much less than c, we can write the relationship seen in Fig. 2.2 as

$$cz \approx v = H_0 r \tag{2.5}$$

where we have chosen to rewrite the luminosity distance D_L as the radial distance r away from us, z is the redshift, and H_0 is a proportionality constant between the receding radial velocity and the distance to that object. Eq. 2.5 is known as Hubble's Law, after the astronomer Edwin Hubble who initially discovered this relationship [Kir04]. The proportionality constant H_0 is the Hubble constant with units of inverse time, but is most usefully written as

$$H_0 = 100\, h\ km\, s^{-1}\, Mpc^{-1} \tag{2.6}$$

where h is a dimensionless parameterization constant depending on current measurements. Hubble's Law states that as you increase in distance you have a corresponding increase in radial velocity (and therefore redshift) of the objects observed. The importance of the Hubble constant is that it emphasizes the constant rate of increase in the graph as the rate of change of space (or "stretching") in km/s per megaparsec of space [Hog99][Kir04]. This may seem odd, but Eq. 2.4 and Eq. 2.5 state that with increasing radial velocity and distance there is also a corresponding increase in the observed redshift, which is due to further objects having traveled longer through a stretching space. Thus, the Hubble constant H_0 measures the current rate of expansion of the universe.
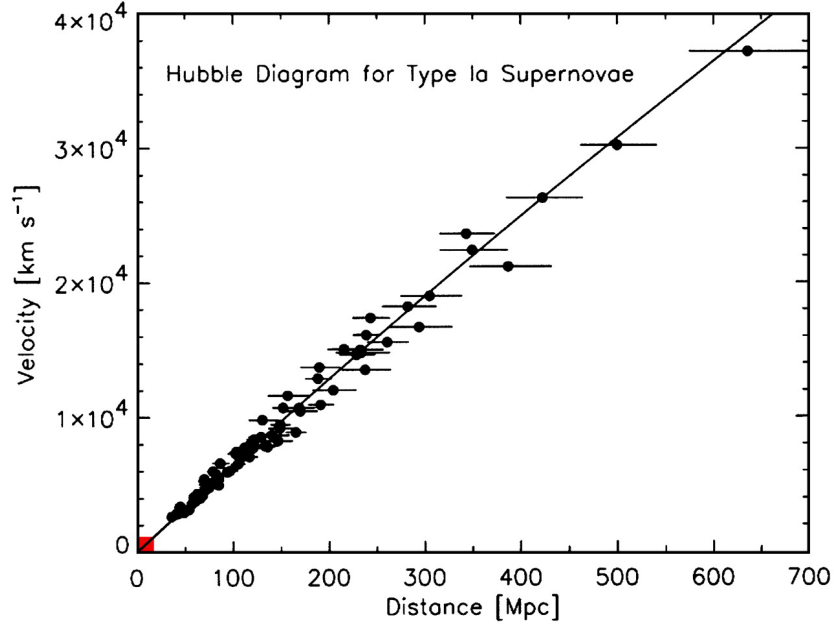
Figure 2.2: Hubble Diagram for Type Ia Supernovae [Kir04]. The linear relationship between velocity and distance is described by Hubble's law, where the slope is the Hubble constant H_0 in $km\,s^{-1}\,Mpc^{-1}$. The scatter in the distance is associated with a statistical error of $< 10\%$ per object measured, with the error increasing with distance. The small red box in the bottom left corner corresponds to the window size of Edwin Hubble's original measurements in 1929.

Efforts to accurately measure the Hubble constant are significantly improved by standard candles like Type 1a supernovae (as seen in Fig. 2.2), but due to their rarity these measurements must be combined with other methods to improve the overall value of H_0 [NRT$^+$16][RMH$^+$16][KH15][RSC$^+$07]. Estimates place bounds on the Hubble parameter h within the range of 0.65 and 0.8, while recent progress in measuring H_0 by Riess et al. (2016) give an estimate of 73.24 $\pm$ 1.74 $kms^{-1}Mpc^{-1}$ with a 2.4% uncertainty in the measurement [RMH$^+$16]. For challenges and tension in estimating the current Hubble constant I encourage the

reader to review José Luis Bernala et al. (2016), "The trouble with H_0", for a more comprehensive overview outside the scope of this thesis [BVR16].

2.0.4   Peculiar Velocity

The relationship described by Hubble's Law in Eq. 2.5 is a model for an idealized isotropic cosmological expansion where galactic objects are stationary with only relative motion due to expansion [Hog99]. From this ideal model you can then estimate the redshift solely due to expansion, known as the cosmological redshift, from $z_{cos} \equiv z = H_0 r/c$. This model, however, neglects the intrinsic motion of galaxies due to gravitational attraction and/or residual momentum gained from the Big Bang [FHW08][WF07]. These are seen as fluctuations in the radial velocity about the ideal expansion line in Fig. 2.2 as expressed by an ideal Hubble's law. The deviations in the observed redshift from the ideal expansion model are actually measurements of the Doppler redshift due to intrinsic galactic motion [Hog99][Car01]. We can account for the deviations in Hubble's law as an additional velocity term due to the intrinsic motion such that

$$cz_{obs} = H_0 r + v_p \tag{2.7}$$

where z_{obs} is the observed redshift and v_p is the *peculiar velocity*, where peculiar implies intrinsic or unique to that object. The peculiar velocity v_p of an astronomical object can be calculated from

$$v_p = \frac{c\left(z_{obs} - z_{cos}\right)}{\left(1 + z_{cos}\right)} \tag{2.8}$$

where z_{obs} is the observed redshift and z_{cos} is the cosmological redshift [Hog99]. Using the idealized form of Hubble's law from Eq. 2.5 we can include the distance r, since z_{cos} is not directly observable, such that Eq. 2.8 can be rewritten as

$$v_p = \frac{cz_{obs} - H_0\,r}{1 + H_0\,r/c} \approx \frac{cz_{obs} - H_0\,r}{1 + z_{obs}} \tag{2.9}$$

where we have made the (reasonable) assumption that $v_p \ll H_0 r$ such that $z_{obs} \approx z_{cos}$. [WF15a][WF15b]. However, Eq. 2.8 is a useful tool for visualizing how we discriminate between cosmological redshift and the Doppler redshift in peculiar velocity calculations.

2.0.5   Cosmic scales

An important limitation on Hubble's law from Eq. 2.4 states that the radial velocity must be much less than the speed of light. Since the radial velocity is the

sum of the cosmological expansion $H_0 r$ and the peculiar velocity v_p, this places a few limitations on the quantities we can calculate. This is because we know that the radial velocity is proportional to the redshift in the spectra of a distant object, and thus if the observed redshift becomes too large then the approximation held by Eq. 2.4 is no longer valid. Such calculations at high redshifts using this method thus inherently introduce distortions in the radial velocity, with estimates placing the limit on the redshift at $z < 2$ before corrections are needed [KH15]. Since radial velocity is also proportional to the distance of an object, the same reasoning can be used to set limits on the distance. Fortunately, in this thesis we will be working with scales well within the boundaries of $v \ll c$ and $z < 2$. I define these scales below explicitly in terms of distance and size.

On very small scales, on the order of magnitude of individual galaxies ($\sim$10 kpc) the motion due to cosmic expansion is small compared to the peculiar motion. At this scale, the motion that dominates is due to gravitational attraction pulling objects towards regions of higher density. Even at small scales of the size of clusters ($\sim$5 $h^{-1} Mpc$), motion towards regions of higher density dominate such that peculiar motion of a cluster tends to be on the same scale as the cosmic expansion. At the larger scales that we are interested in ($\sim$100 $h^{-1} Mpc$), you can think of the Earth as being at the center of an immense sphere with a multitude of clusters and individual galaxies moving around with their own peculiar velocities. At this scale, the motion is almost entirely dominated by the cosmic expansion with the sphere having a very small peculiar motion (a sum of all the motion within the sphere) known as the bulk flow [FHW08][WF15a]. The bulk flow provides us with great insight into the origin and evolution of our universe through the directionality and motion [WF07][WFH09][MFF$^+$12]. In thesis we will be concerning ourselves with radial and peculiar velocity measurements relative to these scales.

2.0.6 *Cosmicflows-3* Database

For our study of peculiar velocities we will be using distance measurements from the *Cosmicflows-3* (CF3) compendium, which is a collection of various observational surveys of 17,669 individual galaxies (see Fig. 2.3) [TCS16]. Each galaxy distance is measured and calibrated amongst different sources and surveys such as Type Ia supernovae observations, infrared photometry of galaxy rotation, Cepheid variables photometry, and estimating the tip of the red giant branch. The galaxies are organized into groups of similar distances; for example, the Virgo Cluster, the largest group, consists of 161 individual galaxy measurements. The compendium provides 11,508 groups organized in this manner, but nearly every group contain less than ten galaxies and 9804 groups are denoted as "singles" due to containing only one galaxy. Despite the limited amount of groups with more than two galaxies, this is a significant improvement to its predecessor *Cosmicflows-2* which

contained only 8,188 individual galaxy entries in total [TCD$^+$13]. The distances (and the observed redshift) provided by *Cosmicflows-3* allows us to calculate the peculiar velocity for both individual galaxies as well as groups.
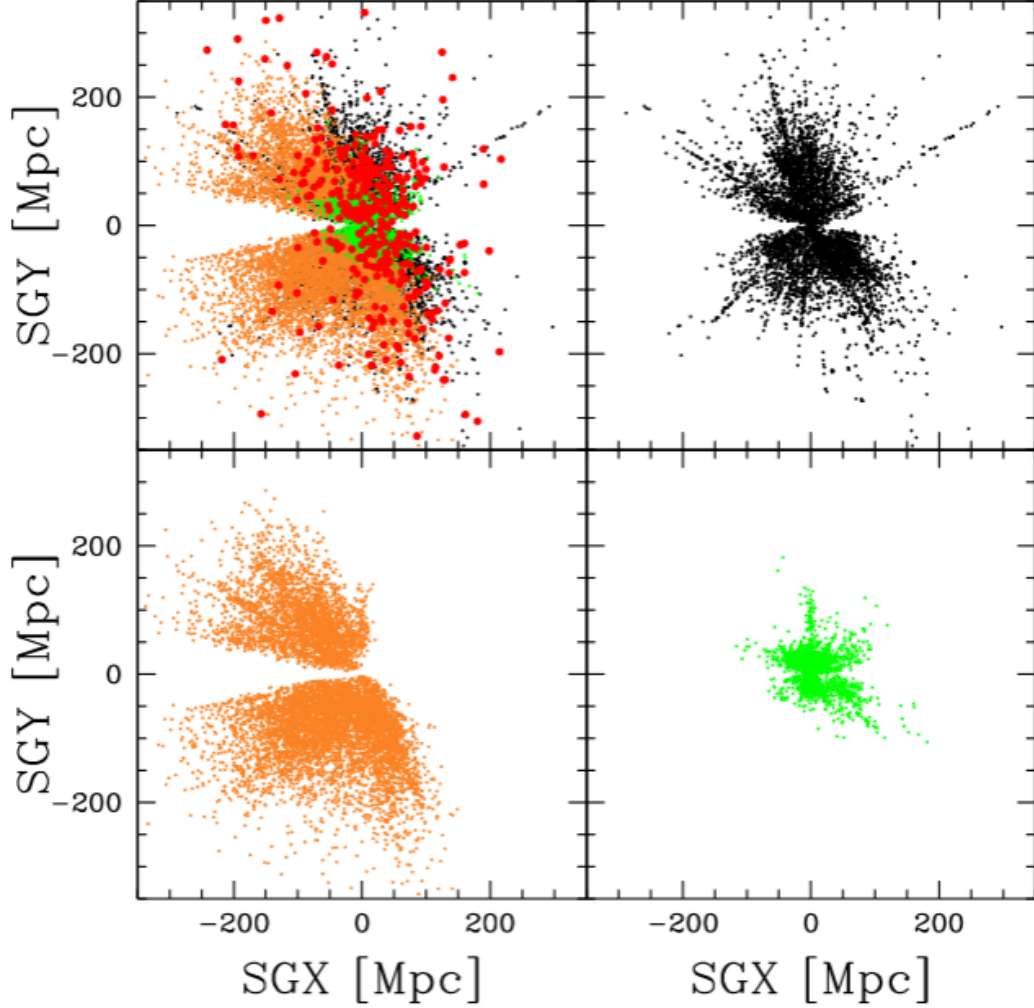
Figure 2.3: Distances of Individual Galaxies in the *Cosmicflows-3* (CF3) Database Projected on Supergalactic SGX-SGY planes [TCS16]. Upper right: distances from the precursor *Cosmicflows-2* compendium in black [TCD+13], Bottom Left: distances from Six Degree Field Galaxy Survey (6dFGS) of the Fundamental Plane in orange, Bottom Right: distances from the Splitzer Space Telescope infrared measurements of galaxy rotation in green. Upper left: all galaxies from different measurement surveys included in CF3 projected on one plane as well as distance measurements from Type 1a supernovae in red.

3 Theory: Method for Measuring Correlation in the Velocity Covariance Matrix (title is a work in progress)

In this section I will be writing about how we will be measuring correlation of peculiar velocities using a new method we are developing in this thesis. We begin with a given a set of distance and redshift measurements, from which we can calculate the peculiar velocity of each object as detailed in the background. We can then organize these measurements to represent a velocity field $v(r)$ where we can use the galaxies to trace the large-scale motion. Performing the Fourier transform of the peculiar velocity field allows us to measure the velocity power spectrum of the field. Since the velocity power spectrum is directly related to the density power spectrum, we can observe large-scale perturbations in the density spectrum and identify their origin. Since the density power spectrum relies on cosmological parameters, to estimate the bulk flow we must perform a likelihood analysis on the value of the cosmological parameters Ω_m, h and Ω_b based on on our peculiar velocity field data. The likelihood function involves a velocity covariance matrix for each peculiar velocity in the field. The method used in the past weighted the contribution of peculiar velocities to the bulk flow based on which scales they probe as measured in the velocity power spectrum. This method was useful in reducing the influence of small scale motions, but the bulk flow they measured disagreed with the value estimated from the standard cosmological model (ΛCDM model) using the cosmic microwave background (CMB) data. Thus, we will be reassessing the inclusion of the small-scale influences by using the velocity covariance matrix to probe the best cosmological parameters that match the data for measuring the bulk flow.

4   Data Analysis and Modeling

In this section I will be using the *Cosmicflows-3* (CF3) distance and redshift values to put our theory into effect! Below is a running list on how we will do this based on the theory in Chapter 3:

- We will calculate the peculiar velocity field

- Perform a Fourier transform on our data

- Measure the velocity and density power spectrum

- Calculate the velocity covariance matrix (i.e. the correlations)

- We will determine various maximum likelihood parameters based on the inclusion of the velocity correlations.

5 Results

In our results section we will determine which cosmological model best matches the velocity correlations present in the CF3 catalog using the velocity covariance matrix.

In our discussion/conclusion sections we will identify if disagreement is still found between our findings and the CMB data. If disagreement does exist and a plausible explanation for this disagreement can't be produced, then this would suggest a need to re-evaluate the current standard model. Personally, I hope that we find that our new method is consistent with the standard model as this would provide a valuable tool in understanding large scale motion. However, regardless of the results, we will either find a more suitable method for measuring the bulk flow or another method that despite taking small-scale influences into account still doesn't align with the standard model.

Bibliography

[BT92]   D. Branch and G. A. Tammann, *Type IA supernovae as standard candles*, Annual review of astronomy and astrophysics **30** (1992), 359–389.

[BVR16]   J. L. Bernal, L. Verde, and A. G. Riess, *The trouble with H_0*, Journal of Cosmology and Astroparticle Physics **10** (2016), 019.

[Car01]   Sean M. Carroll, *The cosmological constant*, Living Reviews in Relativity **4** (2001), no. 1.

[FHW08]   H. A. Feldman, M. J. Hudson, and R. Watkins, *Cosmic Flows on 100 Mpc/h scales*, Conference proceedings for the 43rd Rencontres de Moriond (La Thuile, Val d'Aosta, Italy), Thï¿$\frac{1}{2}$ Gioi Publishers, 2008.

[GP95]   A. Goobar and S. Perlmutter, *Feasibility of Measuring the Cosmological Constant Lambda and Mass Density Omega Using Type IA Supernovae*, The Astrophysical Journal **450** (1995), 14.

[Hog99]   D. W. Hogg, *Distance measures in cosmology*, ArXiv Astrophysics e-prints (1999).

[KGC$^+$05] Kevin Krisciunas, Peter M. Garnavich, Peter Challis, Jose Luis Prieto, Adam G. Riess, Brian Barris, Claudio Aguilera, Andrew C. Becker, Stephane Blondin, Ryan Chornock, Alejandro Clocchiatti, Ricardo Covarrubias, Alexei V. Filippenko, Ryan J. Foley, Malcolm Hicken, Saurabh Jha, Robert P. Kirshner, Bruno Leibundgut, Weidong Li, Thomas Matheson, Anthony Miceli, Gajus Miknaitis, Armin Rest, Maria Elena Salvo, Brian P. Schmidt, R. Chris Smith, Jesper Sollerman, Jason Spyromilio, Christopher W. Stubbs, Nicholas B. Suntzeff, John L. Tonry, and W. Michael Wood-Vasey, *Hubble space telescope observations of nine high-redshift essence supernovae*, The Astronomical Journal **130** (2005), no. 6, 2453.

[KH15]   Nick Kaiser and Michael J. Hudson, *On the perturbation of the luminosity distance by peculiar motions*, Monthly Notices of the Royal Astronomical Society **450** (2015), no. 1, 883–895.

[Kir04]   R. P. Kirshner, *Hubble's diagram and cosmic expansion*, Proceedings of the National Academy of Science **101** (2004), 8–13.

[Kra98]   M. A. Kramer, *An Introduction to Field Analysis Techniques: The Power Spectrum and Coherence*, PDF file (711kB), Society for Neuroscience: The Science of Large Data Sets, 2013 Short Course II, `https://www.sfn.org/~/media/SfN/Documents/Short%20Courses/2013%20Short%20Course%20II/SC2%20Kramer.ashx`, 1998.

[KRA+08]   M. Kowalski, D. Rubin, G. Aldering, R. J. Agostinho, A. Amadon, R. Amanullah, C. Balland, K. Barbary, G. Blanc, P. J. Challis, A. Conley, N. V. Connolly, R. Covarrubias, K. S. Dawson, S. E. Deustua, R. Ellis, S. Fabbro, V. Fadeyev, X. Fan, B. Farris, G. Folatelli, B. L. Frye, G. Garavini, E. L. Gates, L. Germany, G. Goldhaber, B. Goldman, A. Goobar, D. E. Groom, J. Haissinski, D. Hardin, I. Hook, S. Kent, A. G. Kim, R. A. Knop, C. Lidman, E. V. Linder, J. Mendez, J. Meyers, G. J. Miller, M. Moniez, A. M. Mourï¿$\frac{1}{2}$o, H. Newberg, S. Nobili, P. E. Nugent, R. Pain, O. Perdereau, S. Perlmutter, M. M. Phillips, V. Prasad, R. Quimby, N. Regnault, J. Rich, E. P. Rubenstein, P. Ruiz-Lapuente, F. D. Santos, B. E. Schaefer, R. A. Schommer, R. C. Smith, A. M. Soderberg, A. L. Spadafora, L.-G. Strolger, M. Strovink, N. B. Suntzeff, N. Suzuki, R. C. Thomas, N. A. Walton, L. Wang, W. M. Wood-Vasey, and J. L. Yun, *Improved cosmological constraints from new, old, and combined supernova data sets*, The Astrophysical Journal **686** (2008), no. 2, 749.

[MFF+12]   E. Macaulay, H. A. Feldman, P. G. Ferreira, A. H. Jaffe, S. Agarwal, M. J. Hudson, and R. Watkins, *Power spectrum estimation from peculiar velocity catalogues*, Monthly Notices of the Royal Astronomical Society **425** (2012), no. 3, 1709–1717.

[Moo12]   T. A. Moore, *A general relativity workbook*, University Science Books, `http://www.uscibooks.com/moore.htm`, 2012.

[NRT+16]   G. Narayan, A. Rest, B. E. Tucker, R. J. Foley, W. M. Wood-Vasey, P. Challis, C. Stubbs, R. P. Kirshner, C. Aguilera, A. C. Becker, S. Blondin, A. Clocchiatti, R. Covarrubias, G. Damke, T. M. Davis, A. V. Filippenko, M. Ganeshalingam, A. Garg, P. M. Garnavich, M. Hicken, S. W. Jha, K. Krisciunas, B. Leibundgut, W. Li, T. Matheson, G. Miknaitis, G. Pignata, J. L. Prieto, A. G. Riess, B. P. Schmidt, J. M. Silverman, R. C. Smith, J. Sollerman, J. Spyromilio, N. B. Suntzeff, J. L. Tonry, and A. Zenteno, *Light curves of 213 type ia*

supernovae from the essence survey, The Astrophysical Journal Supplement Series **224** (2016), no. 1, 3.

[RMH+16] A. G. Riess, L. M. Macri, S. L. Hoffmann, D. Scolnic, S. Casertano, A. V. Filippenko, B. E. Tucker, M. J. Reid, D. O. Jones, J. M. Silverman, R. Chornock, P. Challis, W. Yuan, P. J. Brown, and R. J. Foley, *A 2.4% determination of the Local Value of the Hubble Constant*, The Astrophysical Journal **826** (2016), no. 1, 56.

[RSC+07] Adam G. Riess, Louis-Gregory Strolger, Stefano Casertano, Henry C. Ferguson, Bahram Mobasher, Ben Gold, Peter J. Challis, Alexei V. Filippenko, Saurabh Jha, Weidong Li, John Tonry, Ryan Foley, Robert P. Kirshner, Mark Dickinson, Emily MacDonald, Daniel Eisenstein, Mario Livio, Josh Younger, Chun Xu, Tomas Dahlï¿½$\frac{1}{2}$n, and Daniel Stern, *New hubble space telescopes discoveries of type ia supernovae at $z \geq 1$: Narrowing constraints on the early behavior of dark energy*, The Astrophysical Journal **659** (2007), no. 1, 98.

[Sha95] H. Shatkay, *The Fourier Transform - A Primer*, Technical Report CS-95-37, PDF (262kB), Department of Computer Science, Brown University, `http://www.phys.hawaii.edu/~jgl/p274/fourier_intro_Shatkay.pdf`, 1995.

[Spe] *Redshifts of quasi-stellar objects*, https://www.noao.edu/image_gallery/html/im0566.html.

[STA16] *STAT 504: Analysis of Discrete Data, Sections 1.4, Likelihood and LogLikelihood*, Course materials on the World Wide Web, Department of Statistics Online Program, Pennsylvania State University, `https://onlinecourses.science.psu.edu/stat504/node/27`, 2016.

[TCD+13] R. Brent Tully, Hï¿½$\frac{1}{2}$lï¿½$\frac{1}{2}$ne M. Courtois, Andrew E. Dolphin, J. Richard Fisher, Philippe Hï¿½$\frac{1}{2}$raudeau, Bradley A. Jacobs, Igor D. Karachentsev, Dmitry Makarov, Lidia Makarova, Sofia Mitronova, Luca Rizzi, Edward J. Shaya, Jenny G. Sorce, and Po-Feng Wu, *Cosmicflows-2: The data*, The Astronomical Journal **146** (2013), no. 4, 86.

[TCS16] R. B. Tully, H. M. Courtois, and J. G. Sorce, *Cosmicflows-3*, The Astronomical Journal **152** (2016), no. 2, 50.

[WF07] R. Watkins and H. A. Feldman, *Power spectrum shape from peculiar velocity data*, Monthly Notices of the Royal Astronomical Society **379** (2007), no. 1, 343–348.

[WF15a]   Richard Watkins and Hume A. Feldman, *Large-scale bulk flows from the cosmicflows-2 catalogue*, Monthly Notices of the Royal Astronomical Society **447** (2015), no. 1, 132–139.

[WF15b]   _____, *An unbiased estimator of peculiar velocity with gaussian distributed errors for precision cosmology*, Monthly Notices of the Royal Astronomical Society **450** (2015), no. 2, 1868–1873.

[WFH09]   Richard Watkins, Hume A. Feldman, and Michael J. Hudson, *Consistently large cosmic flows on scales of 100 h^{-1} Mpc: a challenge for the standard ΛCDM cosmology*, Monthly Notices of the Royal Astronomical Society **392** (2009), no. 2, 743–756.